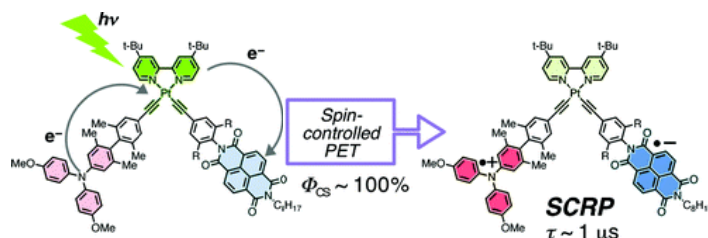


- Highly Efficient Photoproduction of Charge-Separated States in Donor–Acceptor-Linked Bis(acetylide) Platinum Complexes

Suzuki, S.; Sugimura, R.; Kozaki, R.; Keyaki, K.; Nozaki, K.; Ikeda, N.; Akiyama, K.; Okada, K. *J. Am. Chem. Soc.* **2009**, *131*, 10374–10375.

Abstract:

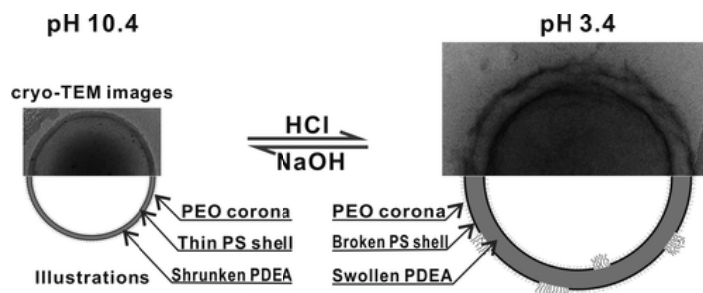


We report a highly efficient charge separation system, D–Pt–A, where D (triphenylamine) and A (naphthalenediimide) are bonded to the Pt moiety through highly twisted phenylene ethynylene linkages. The quantum yields for the formation of the charge-separated state were determined to be nearly unity. The lifetimes of D⁺–Pt–A[–] were $\sim 1 \mu\text{s}$ at room temperature and much longer at low temperature. The spin-correlated radical ion pair was directly observed by means of time-resolved EPR spectroscopy.

- “Breathing” Vesicles

Yu, S.; Azzam, T.; Rouiller, I.; Eisenberg, A. *J. Am. Chem. Soc.* **2009**, *131*, 10557–10566.

Abstract:



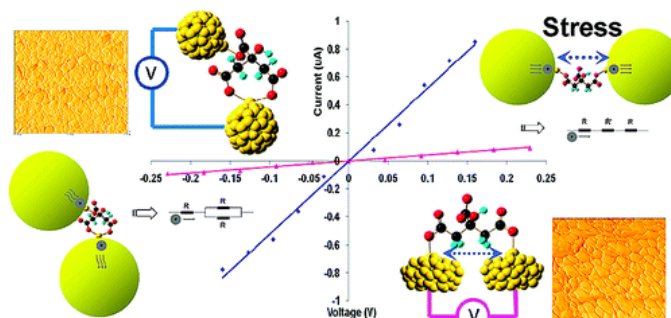
A vesicle system is described that possesses a pH-induced “breathing” feature and consists of a three-layered wall structure. The “breathing” feature consists of a highly reversible vesicle volume change by a factor of ca. 7, accompanied by diffusion of species into and out of the vesicles with a relaxation time of ca. 1 min. The triblock copolymer poly(ethylene oxide)₄₅-block-polystyrene₁₃₀-block-poly(2-diethylaminoethyl methacrylate)₁₂₀ (PEO₄₅-b-PS₁₃₀-b-PDEA₁₂₀) was synthesized via ATRP. Self-assembly into vesicles was carried out at a pH of ca. 10.4. The vesicle wall was shown by cryo-TEM to consist of a sandwich of two external ca. 4 nm thick continuous PS layers and one ca. 17 nm thick PDEA layer in the middle. As the pH decreases, both the vesicle size and the thickness of all three layers increase. The increase of the thickness of the intermediate PDEA layer arises from the protonation and hydration, but the swelling is constrained by the PS layers. The increase of the thickness of the two PS layers is a result of an increasing incompatibility and an accompanying sharpening of the interface between the PS layers and the PDEA layer. Starting at a pH slightly below 6, progressive swelling of the PDEA layer with decreasing pH induces a cracking of the two PS layers and also a sharp increase of the vesicle size and the wall thickness. By pH 3.4, the vesicle size has increased by a factor of ~ 1.9 and the wall shows a cracked surface. These changes between pH 10.4 and 3.4 are highly reversible with the relaxation time of ca. 1 min and can be performed repeatedly.

The change in the wall structure not only increases dramatically the wall permeability to water but also greatly expands the rate of proton diffusion from practically zero to extremely rapid.

- Switchable Molecular Conductivity

Wang, K.; Rangel, N. L.; Kundu, S.; Sotelo, J. C.; Tovar, R. M.; Seminario, J. M.; Liang, H. J. *Am. Chem. Soc.* **2009**, *131*, 10447–10451.

Abstract:

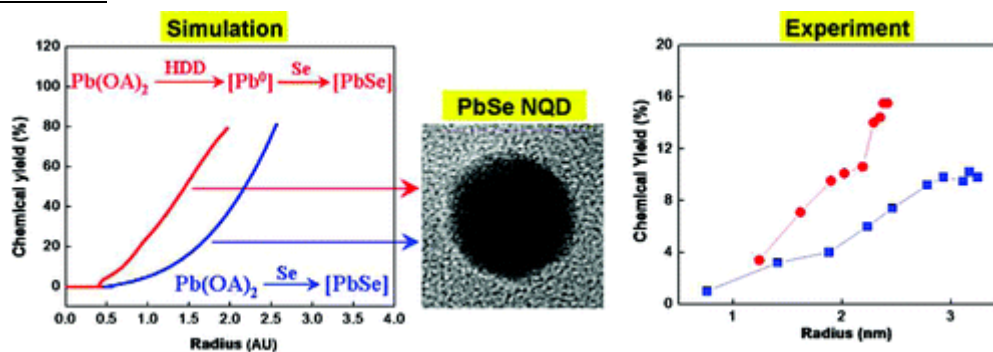


We demonstrate the switchability of the molecular conductivity of a citrate. This was made possible through mechanical stretching of two conformers of such citrate capped on and linked between gold nanoparticles (AuNPs) self-assembled as a film. On the basis of experimental results, theoretical analysis was conducted using the density function theory and Green's function to study the electron flux in the backbone. We found that the molecular conductivity depended on the pathways of electrons that were controlled by the applied mechanical stress. Under stress, we could tune the conductivity up and down for as much as 10-fold. The mechanochemistry behind this phenomenon is an alternative branch of chemistry.

- A Reduction Pathway in the Synthesis of PbSe Nanocrystal Quantum Dots

Joo, J.; Pietryga, J. M.; McGuire, J. A.; Jeon, S.-H.; Williams, D. J.; Wang, H.-L.; Klimov, V. I. *J. Am. Chem. Soc.* **2009**, *131*, 10620–10628.

Abstract:

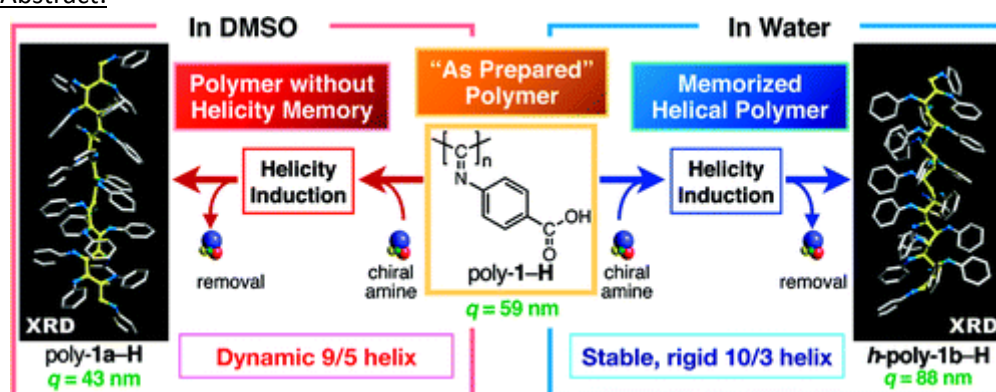


Colloidal nanocrystal quantum dots (NQDs) of narrow band gap materials are of substantial general interest because of their unparalleled potential as infrared fluorophores. While PbSe NQDs are a promising class of infrared-active nanocrystals due to high emission quantum yields and a wide useful spectral range, typical synthetic methods are sensitive to a variety of factors, including the influence of solvent/ligand impurities that render reproducibility difficult. In this work, we specifically examine the effects of diphenylphosphine and 1,2-hexadecanediol, as surrogates for putative trioctylphosphine-based reducing impurities, on the synthesis of PbSe NQDs. Specifically, we compare their influence on NQD size, chemical yield, and photoluminescence quantum yield. While both

additives substantially increase the chemical yield of the synthesis, they demonstrate markedly different effects on emission quantum yield of the product NQDs. We further examine the effects of reaction temperature and oleic acid concentration on the diol-assisted synthesis. Increased oleic acid concentration led to somewhat higher growth rates and larger NQDs but at the expense of lower chemical yield. Temperature was found to have an even greater effect on growth rate and NQD size. Neither temperature nor oleic acid concentration was found to have noticeable effects on NQD emission quantum yield. Finally, we use numerical simulations to support the conjecture that the increased yield is likely a result of faster monomer formation, consistent with the activation of an additional reaction pathway by the reducing species.

- Mechanism of Helix Induction in Poly(4-carboxyphenyl isocyanide) with Chiral Amines and Memory of the Macromolecular Helicity and Its Helical Structures
Hase, Y.; Nagai, K.; Iida, H.; Maeda, K.; Ochi, N.; Sawabe, K.; Sakajiri, K.; Okoshi, K.; Yashima, E. *J. Am. Chem. Soc.* **2009**, *131*, 10719–10732.

Abstract:



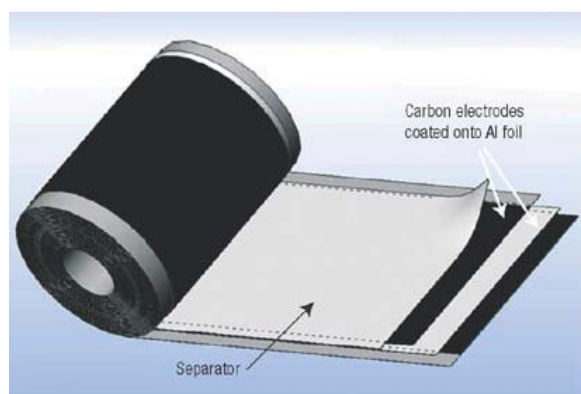
An optically inactive poly(4-carboxyphenyl isocyanide) (poly-1-H) changed its structure into the prevailing, one-handed helical structure upon complexation with optically active amines in dimethylsulfoxide (DMSO) and water, and the complexes show a characteristic induced circular dichroism in the polymer backbone region. Moreover, the macromolecular helicity induced in water and aqueous organic solutions containing more than 50 vol % water could be “memorized” even after complete removal of the chiral amines (*h*-poly-1b-H), while that induced in DMSO and DMSO–water mixtures containing less than 30 vol % water could not maintain the optical activity after removal of the chiral amines (poly-1a-H). We now report fully detailed studies of the helix induction mechanism with chiral amines and the memory of the macromolecular helicity in water and a DMSO–water mixture by various spectroscopic measurements, theoretical calculations, and persistence length measurements together with X-ray diffraction (XRD) measurements. From the spectroscopic results, such as circular dichroism (CD), absorption, IR, vibrational CD, and NMR of poly-1a-H, *h*-poly-1b-H, and original poly-1-H, we concluded that the specific configurational isomerization around the C=N double bonds occurs during the helicity induction process in each solvent. In order to obtain the structural information, XRD measurements were done on the uniaxially oriented films of the corresponding methyl esters (poly-1-Me, poly-1a-Me, and *h*-poly-1b-Me) prepared from their liquid crystalline polymer solutions. On the basis of the XRD analyses, the most plausible helical structure of poly-1a-Me was proposed to be a 9-unit/5-turn helix with two monomer units as a repeating unit, and that of *h*-poly-1b-Me was proposed to be a 10-unit/3-turn helix consisting of one repeating monomer unit. The density functional theory calculations of poly(phenyl isocyanide), a model polymer of *h*-poly-1b-Me, afforded a 7-unit/2-turn helix as the most possible helical structure, which

is in good agreement with the XRD results. Furthermore, the persistence length measurements revealed that these structural changes accompany a significant change in the main-chain stiffness. The mechanism of helix induction in poly-1-H and the memory of the macromolecular helicity are discussed on the basis of these results.

- Materials for electrochemical capacitors

Simon, P.; Gogotsi, Y. *Nature Materials* **2008**, *7*, 845-854.

Abstract:

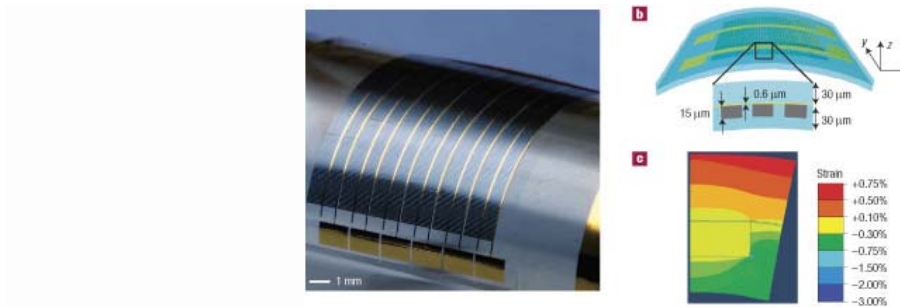


Electrochemical capacitors, also called supercapacitors, store energy using either ion adsorption (electrochemical double layer capacitors) or fast surface redox reactions (pseudo-capacitors). They can complement or replace batteries in electrical energy storage and harvesting applications, when high power delivery or uptake is needed. A notable improvement in performance has been achieved through recent advances in understanding charge storage mechanisms and the development of advanced nanostructured materials. The discovery that ion desolvation occurs in pores smaller than the solvated ions has led to higher capacitance for electrochemical double layer capacitors using carbon electrodes with subnanometre pores, and opened the door to designing high-energy density devices using a variety of electrolytes. Combination of pseudo-capacitive nanomaterials, including oxides, nitrides and polymers, with the latest generation of nanostructured lithium electrodes has brought the energy density of electrochemical capacitors closer to that of batteries. The use of carbon nanotubes has further advanced micro-electrochemical capacitors, enabling flexible and adaptable devices to be made. Mathematical modelling and simulation will be the key to success in designing tomorrow's high-energy and high-power devices.

- Ultrathin silicon solar microcells for semitransparent, mechanically flexible and microconcentrator module designs

Yoon, J.; Baca, A. J.; Park, S.-I.; Elvikis, P.; Geddes, III, J. B.; Li, L.; Kim, R. H.; Xiao, J.; Wang, S.; Kim, T.-H.; Motala, M. J.; Ahn, B. Y.; Duoss, E. B.; Lewis, J. A.; Nuzzo, R. G.; Ferreira, P. M.; Huang, Y.; Rockett, A.; Rogers, J. A. *Nature Materials* **2008**, *7*, 907-915.

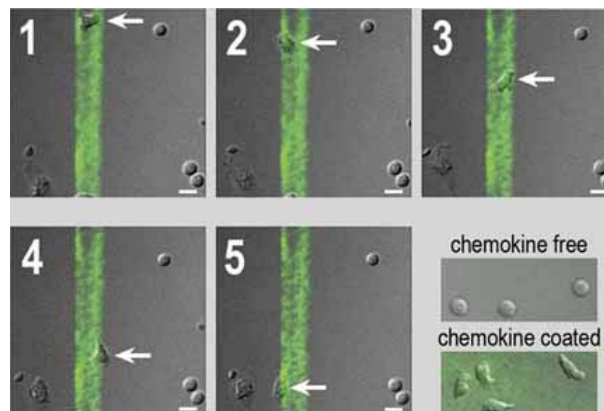
Abstract:



The high natural abundance of silicon, together with its excellent reliability and good efficiency in solar cells, suggest its continued use in production of solar energy, on massive scales, for the foreseeable future. Although organics, nanocrystals, nanowires and other new materials hold significant promise, many opportunities continue to exist for research into unconventional means of exploiting silicon in advanced photovoltaic systems. Here, we describe modules that use large-scale arrays of silicon solar microcells created from bulk wafers and integrated in diverse spatial layouts on foreign substrates by transfer printing. The resulting devices can offer useful features, including high degrees of mechanical flexibility, user-definable transparency and ultrathin-form-factor microconcentrator designs. Detailed studies of the processes for creating and manipulating such microcells, together with theoretical and experimental investigations of the electrical, mechanical and optical characteristics of several types of module that incorporate them, illuminate the key aspects.

- A Biochip Model of Lymphocyte Locomotion on Confined Chemokine Tracks
Buxboim, A.; Geron, E.; Alon, R.; Bar-Ziv, R. *Small* **2009**, *5*, 1723-1726.

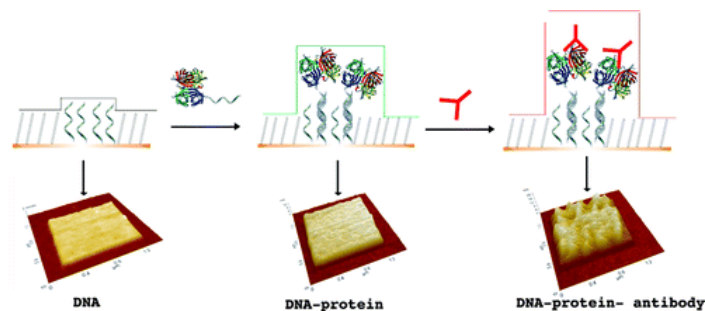
Abstract:



To simulate chemokine tracks presented by narrow stromal networks inside lymph nodes, novel biochips micropatterned with long chemokine stripes are fabricated. Chemokine-coated regions induce T-cell polarization and motility whereas T-cells settling on chemokine-free biochips remain round and static. Chemokine-stimulated T-cell motility is thus directed along patterned stripes.

- Toward Multiprotein Nanoarrays Using Nanografting and DNA Directed Immobilization of Proteins
Bano, F.; Fruk, L.; Sanavio, B.; Glettenberg, M.; Casalis, L.; Niemeyer, C. M.; Scoles, G. *Nano Lett.* **2009**, *9*, 2614–2618.

Abstract:

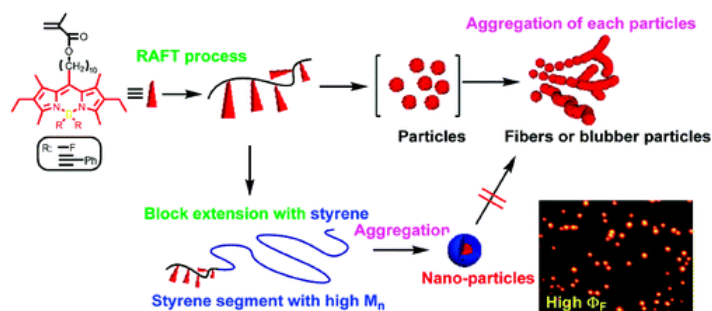


Atomic force microscopy nanografting was utilized to prepare DNA nanopatches of different sizes (200×200 to 1000×1000 nm²) onto which DNA–protein conjugates can be anchored through DNA-directed immobilization. Height measurements were used to assess the binding of the proteins as well as their subsequent interaction with other components, such as antibodies. The results indicate that nanografted patch arrays are well suited for application in biosensing and could enable the fabrication of multifeature protein nanoarrays.

- Highly Luminescent Nanoparticles: Self-Assembly of Well-Defined Block Copolymers by π - π Stacked BODIPY Dyes as Only a Driving Force.

Nagai, A.; Kokado, K.; Miyake, J.; Chujo, Y. *Macromolecules* **2009**, *42*, 5446–5452.

Abstract :

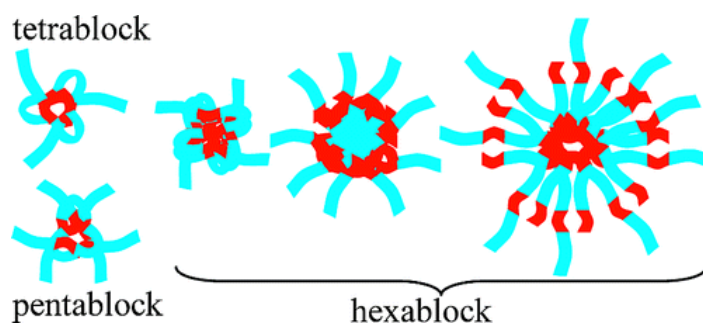


Well-defined polymers incorporated BODIPY dyes into the PMMA side chain, and the block copolymers were synthesized by the RAFT process. The controlled/living character of the polymerization of MMA monomers with pendant BODIPY dyes was confirmed by the formation of the narrow molecular weight distribution products, the linear first-order kinetic plot, linear increase of molecular weight with the conversion, and block extension with styrene. The SEM images of the obtained homopolymers showed micrometer-sized blubber particle- or chain-like structures, which come from the aggregated particles by strong intermolecular π - π stacking of BODIPY dyes. In contrast, the designed block copolymers formed nanoparticles with enhanced luminescence ($\Phi_F > 0.70$) by preventing higher molecular weight polystyrene segment from aggregation by the strong π - π stacking.

- Synthesis and Characterization of Amphiphilic Multiblock Copolymers: Effect of the Number of Blocks on Micellization

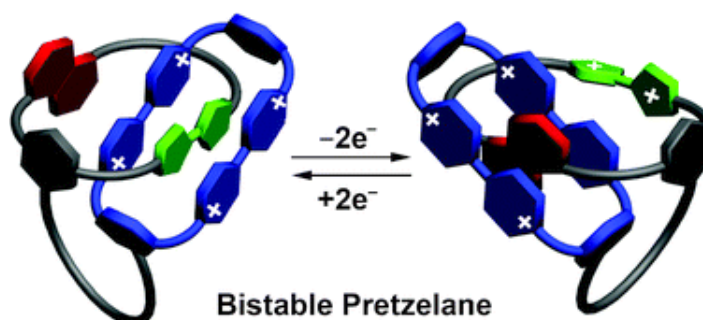
Hadjiantoniou, N. A.; Triftaridou, A. I.; Kafouris, D.; Gradzielski, M.; Patrickios, C. S. *Macromolecules* **2009**, *42*, 5492–5498.

Abstract :



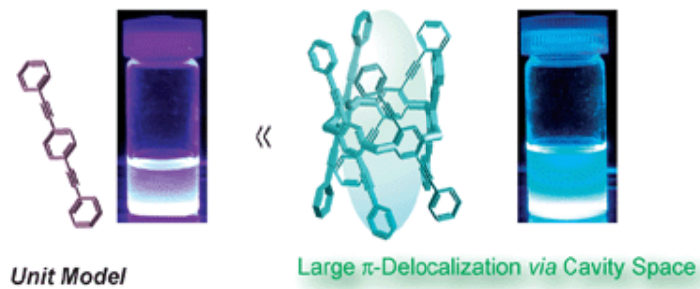
Five linear amphiphilic multiblock copolymers based on 2-(dimethylamino)ethyl methacrylate (“D”) and methyl methacrylate (“M”), bearing from two to six blocks, were synthesized using sequential group transfer polymerization. All copolymers were obtained from the same polymerization flask (by the withdrawal of a sufficient amount of sample and appropriate adjustment of subsequent monomer loadings) to ensure better comparison between the various multiblocks. A theoretical degree of polymerization (DP_{th}) of 20 was targeted for all D blocks, whereas a DP_{th} of 10 was aimed for the M blocks. Upon characterization using gel permeation chromatography and ¹H NMR spectroscopy, the copolymers were confirmed to have the expected values of molecular weights and compositions. Subsequently, the aqueous micellization behavior of these copolymers was probed using dye solubilization, dynamic light scattering, and small-angle neutron scattering. Dye solubilization experiments indicated that micelles readily formed at low copolymer concentrations equal to or less than 0.03% w/w. The scattering measurements revealed that despite the differences in their overall DP_{th} values, the triblock, the tetrablock, and the pentablock copolymers self-assembled in water to form micelles with radii of gyration and hydrodynamic radii very similar to each other, suggesting chain looping and the formation of flowerlike micelles, which is in agreement with recent Monte Carlo simulations.

- A bistable pretzelane
Zhao, Y.-L.; Trabolsi, A.; Stoddart, J. F. *Chem. Commun.* **2009**, 4844 – 4846.
Abstract :



A switchable donor–acceptor pretzelane composed of a crown ether containing tetrathiafulvalene and 1,5-dihydroxynaphthalene recognition units and a covalently tethered cyclobis(paraquat-p-phenylene) ring exhibits unidirectional motion on both oxidation (forwards) and reduction (backwards).

- Through-space -delocalized Pillar[5]arene
Ogoshi, T.; Umeda, K.; Yamagishi, T. A.; Nakamoto, Y. *Chem. Commun.* **2009**, 4874 – 4876.
Abstract:

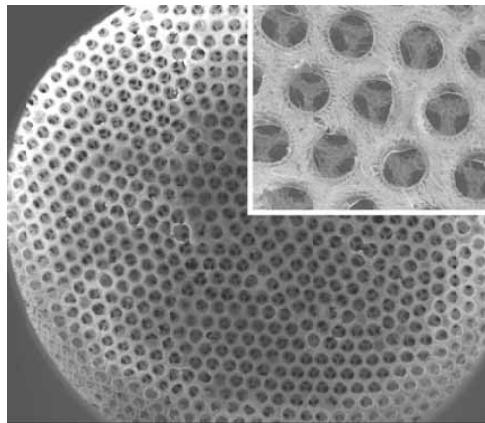


Pillar[5]arene from modified phenylethynyl groups was prepared; since the repeating π -conjugated units were largely π -delocalized via the through-space within the cavity, it showed temperature- and solvent-responsive blue-green emission.

- Chitosan-Based Inverse Opals: Three-Dimensional Scaffolds with Uniform Pore Structures for Cell Culture

Choi, S-W.; Xie, W.; Xia, Y. *Adv. Mater.* **2009**, 2997-3001.

Abstract:

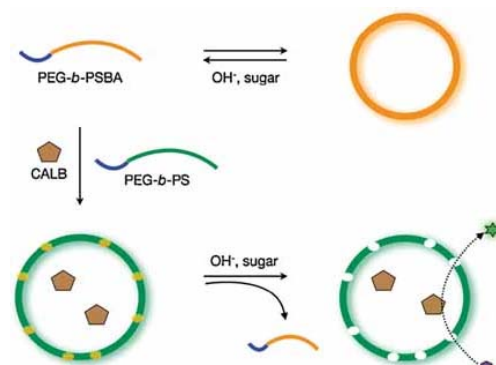


Chitosan inverse opal scaffolds: Three-dimensional chitosan scaffolds with an inverse opal structure have been fabricated using a cubic close packed lattice of polymer beads as the template. The scaffolds have a uniform and interconnected pore structure as well as a fibrous morphology on the wall. They can be used as a model system for in vitro studies of cell culture and as clinically practical scaffolds for tissue engineering.

- A Polymersome Nanoreactor with Controllable Permeability Induced by Stimuli-Responsive Block Copolymers

Kim, K. T.; Cornelissen, J. J. L. M.; Nolte, R.J.M. van Hest J. C. M. *Adv. Mater.* **2009**, 2787-2791.

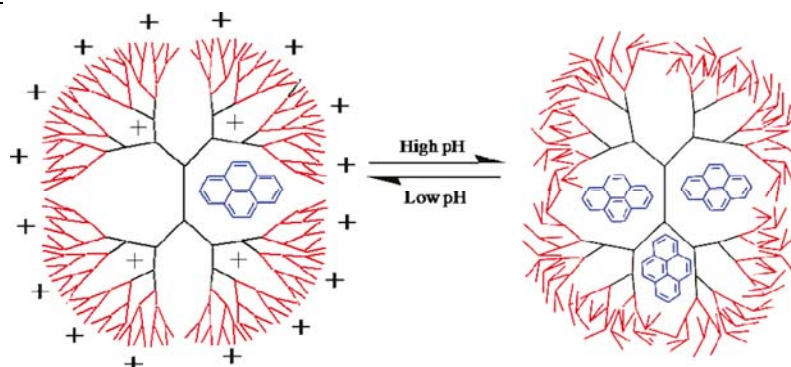
Abstract:



A method to generate and control the permeability of polymersome membranes using mixtures of amphiphilic and stimuli-responsive boronic acid-containing block copolymers is reported. The latter block copolymers form phase-separated domains in the polymersomes, which can be dissolved by increasing the pH of the medium or by introducing sugar molecules that covalently bind to the boronic acid moieties.

- pH-Dependent Encapsulation of Pyrene in PPI-Core:PAMAM-Shell Dendrimers
Kannaiyan, D.; Imae, T. *Langmuir* **2009**, *25*, 5282–5285.

Abstract:



Core-shell dendrimers consisting of poly(propyleneimine) (PPI) dendrimer as a core and poly(amidoamine) (PAMAM) dendrons as a shell have been synthesized through the route of Michael addition reaction followed by amidation. These macromolecules were investigated their ability to solubilize a guest molecule, pyrene. The number of encapsulated pyrene molecules per dendrimer increased with pH of a solution and generation (G) of PAMAM dendron, and it reached 2.7 for PPI(G3)-core:PAMAM(G3)-shell dendrimer at pH 11. It was confirmed that the solubilized pyrene located in the hydrophobic nanocavities of the PPI dendrimer core in the dendrimer. The shrunk PAMAM dendron shell should play a role of retention fence of doped molecules.

- Gels for the Conservation of Cultural Heritage
Baglioni, P.; Dei, L.; Carretti, E.; Giorgi, R. *Langmuir* **2009**, *25*, 8373–8374.

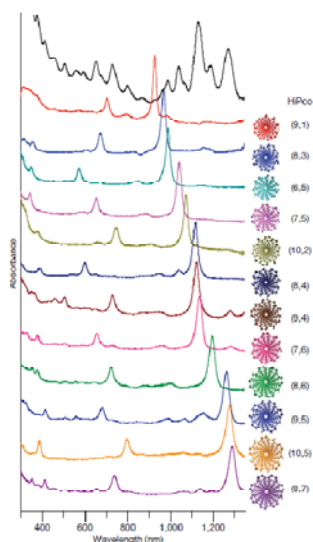
Abstract:



Gels are becoming one of the most important tools for the conservation of cultural heritage. They are very versatile systems and can be easily adapted to the cleaning and consolidation of works of art. This perspective reviews the major achievements in the field and suggests possible future developments.

- DNA sequence motifs for structure-specific recognition and separation of carbon nanotubes
Tu, X.; Manohar, S.; Jagota, A.; Zheng, M ; *Nature* **2009**, *460*, 250-253.

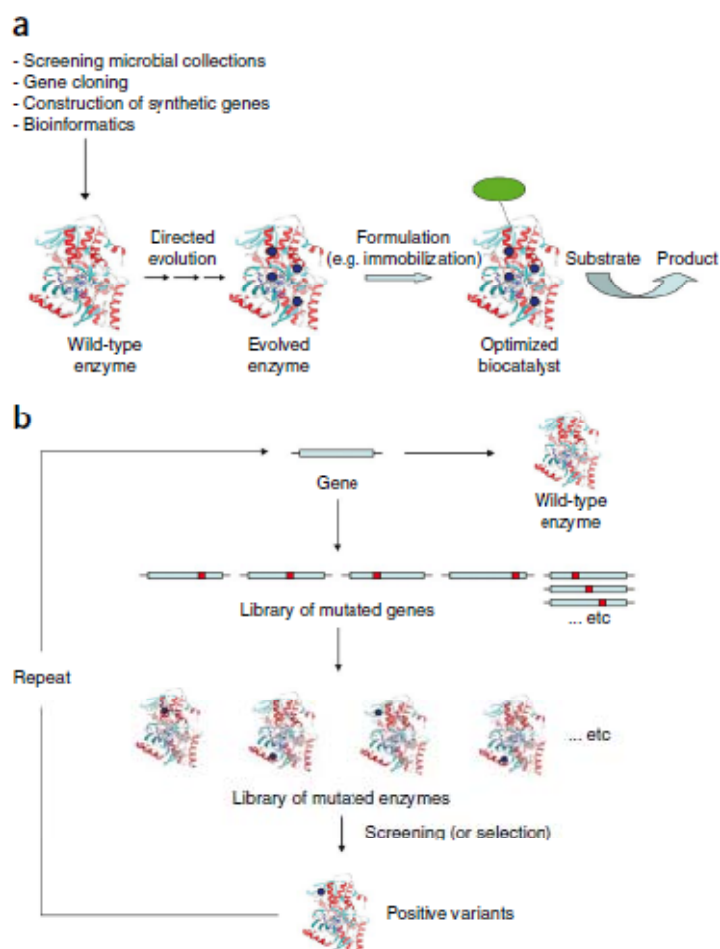
Abstract :



Single-walled carbon nanotubes (SWNTs) are a family of molecules that have the same cylindrical shape but different chiralities¹. Many fundamental studies and technological applications² of SWNTs require a population of tubes with identical chirality that current syntheses cannot provide. The SWNT sorting problem—that is, separation of a synthetic mixture of tubes into individual single-chirality components—has attracted considerable attention in recent years. Intense efforts so far have focused largely on, and resulted in solutions for, a weaker version of the sorting problem: metal/semiconductor separation^{3,4}. A systematic and general method to purify each and every single-chirality species of the same electronic type from the synthetic mixture of SWNTs is highly desirable, but the task has proven to be insurmountable to date. Here we report such a method, which allows purification of all 12 major single-chirality semiconducting species from a synthetic mixture, with sufficient yield for both fundamental studies and application development. We have designed an effective search of a DNA library of 1060 in size, and have identified more than 20 short DNA sequences, each of which recognizes and enables chromatographic purification of a particular nanotube species from the synthetic mixture. Recognition sequences exhibit a periodic purine–pyrimidines pattern, which can undergo hydrogen bonding to form a two-dimensional sheet, and fold selectively on nanotubes into a well-ordered three-dimensional barrel. We propose that the ordered two-dimensional sheet and three-dimensional barrel provide the structural basis for the observed DNA recognition of SWNTs.

- Directed evolution drives the next generation of biocatalysts
Turner, N. J. *Nature Chem. Biol.* **2009**, *5*, 567-573.

Abstract:

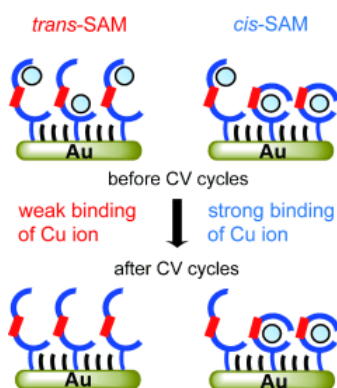


Enzymes are increasingly being used as biocatalysts in the generation of products that have until now been derived using traditional chemical processes. Such products range from pharmaceutical and agrochemical building blocks to fine and bulk chemicals and, more recently, components of biofuels. For a biocatalyst to be effective in an industrial process, it must be subjected to improvement and optimization, and in this respect the directed evolution of enzymes has emerged as a powerful enabling technology. Directed evolution involves repeated rounds of (i) random gene library generation, (ii) expression of genes in a suitable host and (iii) screening of libraries of variant enzymes for the property of interest. Both *in vitro* screening-based methods and *in vivo* selection-based methods have been applied to the evolution of enzyme function and properties. Significant developments have occurred recently, particularly with respect to library design, screening methodology, applications in synthetic transformations and strategies for the generation of new enzyme function.

- Regulating Copper-Binding Affinity with Photoisomerizable Azobenzene Ligand by Construction of a Self-Assembled Monolayer

Takahashi, I.; Honda, Y.; Hirota, S. *Angew. Chem. Int. Ed.* **2009**, *48*, 6065–6068.

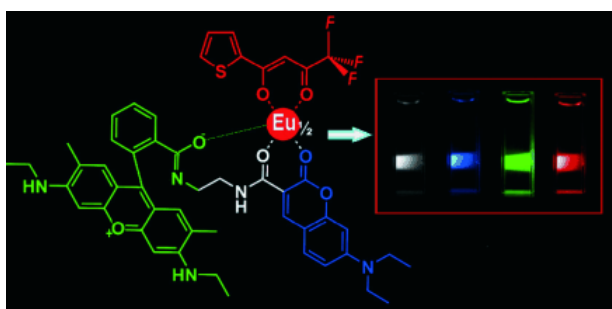
Abstract:



Catch and release! Self-assembled monolayers (SAMs) of both *trans*- and *cis*-azobenzene ligands can bind Cu^{II} ions. Ions bound to the *trans* ligand are released by cyclic voltammetry (CV) redox scans whereas those bound to the *cis* ligand are not (see picture). Irradiation of the *cis*-SAM with visible light leads to removal of the bound Cu ions by *cis*-to-*trans* photoisomerization.

- A Color-Tunable Europium Complex Emitting Three Primary Colors and White Light
He, G.; Guo, D.; He, C.; Zhang, X.; Zhao, X.; Duan, C. *Angew. Chem. Int. Ed.* **2009**, *48*, 6132–6135.

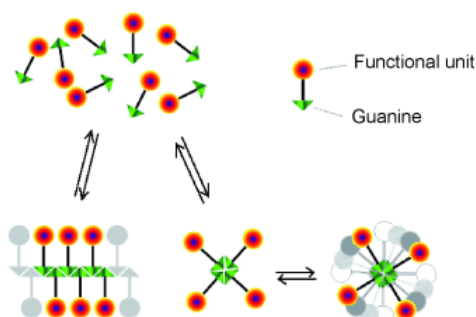
Abstract:



Tunable emission colors are shown by a single-component emitter incorporating an Eu^{III} moiety as the origin of red light and an organic ligand comprising coumarin (blue emission) and Rhodamine 6G (green emission) fluorophores. This dye can emit three individual primary colors (blue, green, and red) as well as nearly pure white light (see picture).

- Guanosine Hydrogen-Bonded Scaffolds: A New Way to Control the Bottom-Up Realisation of Well-Defined Nanoarchitectures
Lena, S.; Masiero, S.; Pieraccini, S.; Spada, G. *P. Chem. Eur. J.* **2009**, *15*, 7792–7806.

Abstract:



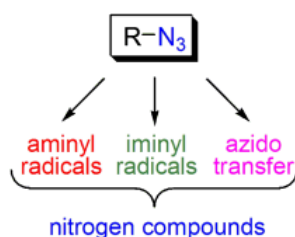
Over the last two decades, guanosine-related molecules have been of interest in different areas, ranging from structural biology to medicinal chemistry, supramolecular chemistry and

nanotechnology. The guanine base is a multiple hydrogen-bonding unit, capable also of binding to cations, and fits very well with contemporary studies in supramolecular chemistry, self-assembly and non-covalent synthesis. This Concepts article, after reviewing on the diversification of self-organised assemblies from guanosine-based low-molecular-weight molecules, will mainly focus on the use of guanine moiety as a potential scaffold for designing functional materials of tailored physical properties.

- From Azides to Nitrogen-Centered Radicals: Applications of Azide Radical Chemistry to Organic Synthesis

Minozzi, M.; Nanni, D.; Spagnolo, P. *Chem. Eur. J.* **2009**, *15*, 7830–7840.

Abstract:



Over the last thirty years organic azides have drawn a great deal of attention as radical traps for carbon- and heteroatom-centered radicals, both in intra- and in intermolecular processes. The resulting intermediates (nitrogen-centered radicals such as triazenyls, aminyls, or even iminyls) can be conveniently employed in the synthesis of a variety of cyclic and acyclic nitrogen-containing compounds.

- Organocatalysis—after the gold rush

Bertelsen, S.; Jørgensen, K. A. *Chem. Soc. Rev.* **2009**, *38*, 2178 – 2189.

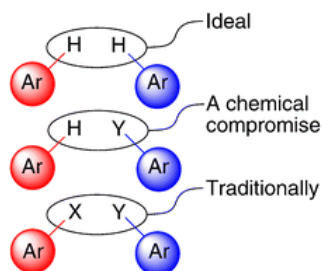
Abstract:



The use of secondary amines as asymmetric catalysts in transformations of carbonyl compounds has seen tremendous development in recent years. Going from sporadic reports of selected reactions, aminocatalysis can now be considered as one of the methods of choice for many asymmetric functionalizations of carbonyl compounds—primarily of aldehydes and ketones. These functionalizations have been published at a breathtaking pace over the last few years—during the “golden age” and “gold rush” of organocatalysis. This *tutorial review* will firstly sketch the basic developments in organocatalysis, focussing especially on the use of secondary amines as catalysts for the functionalization of aldehydes and α,β -unsaturated aldehydes, with emphasis on the mechanisms of the transformations and, secondly, outline recent trends within central areas of this research topic. Lastly, we will present our guesses as to where new developments might take organocatalysis in the years to come.

- Recent advances in aryl–aryl bond formation by direct arylation
McGlacken, G. P.; Bateman, L. M. *Chem. Soc. Rev.* **2009**, *38*, 2447 – 2464.

Abstract:



The abundance of the biaryl structural motif in natural products, in biologically active molecules and in materials chemistry has positioned aryl–aryl (Ar–Ar) bond formation high on the agenda of synthetic chemists. For decades well-known reactions such as the Mizoroki–Heck and Suzuki–Miyaura have been the methods of choice to furnish biaryls. More recently, however, alternative methods, most notably direct arylation *via* C–H activation, have become the focus of many research groups. Compared to traditional methods, direct arylation affords Ar–Ar compounds in fewer steps by removing the need for prefunctionalisation. Furthermore, given that either one or two hydrogens are targeted, less waste and good atom economy are features of this methodology. This *critical review* covers, in the main part, reports from January 1, 2006, to October 22, 2008 (117 references).